Supplementary materials

Exciton engineering based on star-shaped blue thermally activated delayed fluorescence emitters for efficient white organic light-emitting diodes

Zhe Li[1], Chunbo Duan[1*], Ying Li[1], Jing Zhang[1], Chunmiao Han[1], Hui Xu[1*]

[1] Key Laboratory of Functional Inorganic Material Chemistry (Chinese Ministry of Education), Heilongjiang University, 74 Xuefu Road, Harbin 150080, China

Content

Experimental section 2
Thermal Properties 6
Gaussian Simulation Results 7
Steady-State Photophysical Properties 8
Transient Emission Properties 11
Electrical Properties 16
Table S1. Physical properties of *x*DPACPO. 18
Table S2. Photophysical properties of DBFDPO:30% *x*DPACPO films. 18
OLED Performance 19
Table S3. EL performance of TADF WOLEDs based on *x*DPACPO. 25
References 26

Experimental section

Materials and Instruments

^{1}H NMR spectra were recorded using a Varian Mercury plus 400NB spectrometer relative to tetramethylsilane (TMS) as internal standard. Molecular masses were determined by a MALDI-TOF-MS. Elemental analyses were performed on a Vario EL III elemental analyzer. The crystal suitable for single-crystal XRD analysis was obtained through slowly diffusing hexane into dichloromethane solution of **SDPACPO** and **TDPACPO** at room temperature. All diffraction data were collected at 295 K on a Rigaku Xcalibur E diffractometer with graphite monochromatized Mo Kα (λ = 0.71073 Å) radiation in ω scan mode. All structures were solved by direct method and difference Fourier syntheses. Non-hydrogen atoms were refined by full-matrix least-squares techniques on F2 with anisotropic thermal parameters. The hydrogen atoms attached to carbons were placed in calculated positions with C−H = 0.93 Å and U(H) = 1.2Ueq(C) in the riding model approximation. All calculations were carried out with the SHELXL97 program. Absorption and photoluminescence (PL) emission spectra of the target compound were measured using a SHIMADZU UV-3150 spectrophotometer and a SHIMADZU RF-5301PC spectrophotometer, respectively. Thermogravimetric analysis (TGA) and differential scanning calorimetry (DSC) were performed on Shimadzu DSC-60A and DTG-60A thermal analyzers under nitrogen atmosphere at a heating rate of 10 °C min^{-1}. The morphological characteristics of the *vacuum*-evaporated films were measured with an atom force microscope (AFM) Agilent 5100 under the tapping mode. Cyclic voltammetric (CV) studies were conducted using an Eco Chemie B. V. AUTOLAB potentiostat in a typical three-electrode cell with a glassy carbon working electrode, a platinum wire counter electrode, and a silver/silver chloride (Ag/AgCl) reference electrode. All electrochemical experiments were carried out under a nitrogen atmosphere at room temperature in dichloromethane. Phosphorescence spectra were measured in dichloromethane using an Edinburgh FPLS 920 fluorescence spectrophotometer at 77 K cooling by liquid nitrogen with a delay of 300 μs using Time-Correlated Single Photon Counting (TCSPC) method with a microsecond pulsed Xenon light source for 10 μs-10 s lifetime measurement, the synchronization photomultiplier for signal collection and the Multi-Channel Scaling Mode of the PCS900 fast counter PC plug-in card for data processing. The TADF dye doped films (100 nm) were prepared through vacuum evaporation for optical analysis.

Photoluminescence quantum yields (PLQY, η_{PL}) of these films were measured through a labsphere 1-M-2 (ϕ = 6") integrating sphere coated by Benflect with efficient light reflection in a wide range of 200-1600 nm, which was integrated with FPLS 920. The absolute η_{PL} determination of the sample was performed by two spectral (emission) scans, with the emission monochromator scanning over the Rayleigh scattered light from the sample and from a blank substrate. The first spectrum recorded the scattered light and the emission of the sample, and the second spectrum contained the scattered light of Benflect coating. The integration and subtraction of the scattered light parts in these two spectra arrived at the photon number absorbed by the samples (N_a); while, integration of the emission of the samples to calculate the emissive photon number (N_e). Then, the absolute η_{PL} can be estimated according to the equation of $\eta_{PL} = N_e/N_a$. Spectral correction (emission arm) was applied to the raw data after background subtraction, and from these spectrally corrected curves the quantum yield was calculated using aF900 software wizard.

Synthesis

All the reagents used for synthesis were purchased from Alfa and Sinopharm Chemical Reagent Co., Ltd, and used without further purification.

*10-(4-Bromophenyl)-9,9-diphenyl-9,10-dihydroacridine (**DPACPhBr**):* 9,9-diphenyl-9,10-dihydroacridine (DPAC, 3.33 g, 10 mmol), 1-bromo-4-iodobenzene (8.49 g, 30 mmol), K_2CO_3 (2.76 g, 20 mmol) and CuI (0.19 g, 1 mmol) were mixed and stirred at 200 °C for 48 h. Then, the system was quenched with ice water. The mixture was extracted with dichloromethane (DCM, 3 × 20 mL). The combined organic layer was dried over anhydrous Na_2SO_4 and the solvent was removed by evaporation. The crude bromide was purified by flash column chromatography to afford the title compound as white powder with yield of 69%. ^{1}H NMR (TMS, $CDCl_3$, 400 MHz): δ = 7.633 (d, J = 8.4 Hz, 2H), 7.231 (m, 6H), 7.045 (m, 2H); 6.694 (dd, J_1 = 2.4, J_2 = 8.0 Hz, 4H); 6.935 (d, J = 8.4 Hz, 2H), 6.890 (m, 4H), 6.381 ppm (d, J = 8.0 Hz, 2H); LDI-MS: m/z (%): 487 (100) [M^+]; elemental analysis (%) for $C_{31}H_{22}BrN$: C 76.23, H 4.54, N 2.87; found: C 76.24, H 4.53, N 2.91.

General Procedure of Phosphorylation: In Ar, DPACPhBr (16.1 g, 33 mmol) was dissolved in anhydrous THF. The solution was cooled to -78 °C, and then *n*-BuLi (2.5 M in hexane, 13.2 mL, 33 mmol) was added in drop. The mixture was stirred for 2 h -78 °C, and then

diphenylchlorophosphine (5.9 mL, 33 mmol for **SDPACPO**), phenyldichlorophosphine (2.2 mL, 16 mmol for **DDPACPO**), or phosphorus trichloride (1 mL, 11 mmol for **TDPACPO**) was added in drop and stirred at -78 °C for another 1 h. Then, the mixture was gradually warmed to room temperature and stirred for an additional 4 h. The reaction was then quenched by water addition. The mixture was extracted with CH_2Cl_2 (3 × 30 mL). CH_2Cl_2 solution was concentrated to 30 mL and then added by 30% H_2O_2 (6.8 mL, 60 mmol) at 0 °C and stirred for 4 h. The mixture was extracted again with CH_2Cl_2 (3 × 30 mL). The organic phase was combined and dried with anhydrous Na_2SO_4. The solvent was then removed in vacuo. The crude product was purified by flash column chromatography.

*(4-(9,9-Diphenylacridin-10(9H)-yl)phenyl)diphenylphosphine oxide (**SDPACPO**):* yellowish white powder with a yield of 65%. ^{1}H NMR (TMS, $CDCl_3$, 400 MHz): δ = 7.800 (dd, J_1 = 8.4 Hz, J_2 = 11.6 Hz, 2H), 7.728 (dd, J_1 = 7.2 Hz, J_2 = 12.0 Hz, 4H), 7.580 (t, J = 6.6 Hz, 2H), 7.539 (t, J = 7.4 Hz, 4H), 7.239 (m, 6H), 7.155 (dd, J_1 = 2.0 Hz, J_2 = 8.0 Hz, 2H), 7.070 (m, 2H), 6.950 (d, J = 7.6 Hz, 4H), 6.897 (d, J = 4.0 Hz, 4H), 6.444 ppm (d, J = 8.0 Hz, 2H). ^{13}C NMR (TMS, $CDCl_3$, 100 MHz): δ = 146.045, 141.658, 134.359, 134.253, 132.101, 132.003, 131.232, 131.107, 130.551, 130.323, 130.058, 128.830, 128.709, 127.635, 126.905, 126.357, 120.740, 114.377, 56.815 ppm. ^{31}P NMR (TMS, $CDCl_3$, 160 MHz): 29.273 ppm. LDI-MS: m/z (%): 609 (100) [M^+]; elemental analysis (%) for $C_{43}H_{34}NOP$: C 84.71, H 5.29, N 2.30; found: C 84.70, H 5.30, N 2.33. CCDC number: 2101821.

*Bis(4-(9,9-diphenylacridin-10(9H)-yl)phenyl)(phenyl)phosphine oxide (**DDPACPO**):* yellowish white powder with a yield of 51%. ^{1}H NMR (TMS, $CDCl_3$, 400 MHz): δ = 7.829 (dd, J_1 = 8.0 Hz, J_2 = 11.6 Hz, 4H), 7.768 (dd, J_1 = 7.2 Hz, J_2 = 12.0 Hz, 2H), 7.615 (t, J = 6.6 Hz, 1H), 7.545 (t, J = 7.2 Hz, 2H), 7.208 (m, 16H), 7.081 (m, 4H), 6.952 (d, J = 7.6 Hz, 8H), 6.897 (d, J = 3.2 Hz, 8H), 6.444 ppm (d, J = 8.0 Hz, 4H). ^{13}C NMR (TMS, $CDCl_3$, 100 MHz): δ = 146.081, 141.681, 134.387, 134.282, 132.112, 132.013, 131.239, 131.114, 130.355, 130.319, 130.029, 128.695, 128.574, 127.620, 126.891, 126.334, 120.641, 114.275, 56.788 ppm. ^{31}P NMR (TMS, $CDCl_3$, 160 MHz): 28.867 ppm. LDI-MS: m/z (%): 940 (100) [M^+]; elemental analysis (%) for $C_{68}H_{49}N_2OP$: C 86.78, H 5.25, N 2.98; found: C 86.80, H 5.24, N 3.00.

*Tris(4-(9,9-diphenylacridin-10(9H)-yl)phenyl)phosphine oxide (**TDPACPO**):* yellowish white powder with a yield of 50%. ^{1}H NMR (TMS, $CDCl_3$, 400 MHz): δ = 7.853 (dd, J_1 = 8.4 Hz, J_2 = 11.6 Hz, 6H), 7.227 (m, 24H), 7.089 (m, 6H), 6.953 (dd, J_1 = 2.0 Hz, J_2 = 8.0 Hz, 12H), 6.923 (d,

J = 3.2 Hz, 12H), 6.472 ppm (d, J = 8.0 Hz, 6H). ^{13}C NMR (TMS, $CDCl_3$, 100 MHz): δ = 146.013, 141.648, 134.330, 134.225, 131.164, 131.038, 130.809, 130.339, 130.095, 127.659, 126.928, 126.391, 120.858, 114.530, 56.860 ppm. ^{31}P NMR (TMS, $CDCl_3$, 160 MHz): 28.491 ppm. LDI-MS: m/z (%): 1271 (100) [M^+]; elemental analysis (%) for $C_{93}H_{66}N_3OP$: C 87.78, H 5.23, N 3.30; found: C 87.79, H 5.23, N 3.33. CCDC number: 2101822.

Gaussian Calculations

DFT computations were carried out with different parameters for structure optimizations and vibration analyses. The ground state configurations of **SDPACPO** and **TDPACPO** were established according to single crystal data; while, the ground state geometry of **DDPACPO** was generated taking its congeners as reference. The ground states in vacuum were optimized by the restricted and unrestricted formalism of Beck's three-parameter hybrid exchange functional[1] and Lee, and Yang and Parr correlation functional[2] B3LYP/6-31G(d,p), respectively. The fully optimized stationary points were further characterized by harmonic vibrational frequency analysis to ensure that real local minima had been found without imaginary vibrational frequency. The total energies were also corrected by zero-point energy both for the ground state and triplet state. Natural transition orbital (NTO) analysis was performance based on time-dependent DFT (TD-DFT) method, which was based on ground-state geometries. The contours were visualized with Gaussview 5.0. All computations were performed using the Gaussian 09 package. [3]

OLED fabrication

ITO substrate was cleaned and loaded into a deposition chamber. After treating with oxygen plasma for 3 min, devices were fabricated layer-by-layer through evaporation at a pressure below 4×10^{-4} Pa. Deposition rates are 0.1-0.2 nm s^{-1} for organic layers, 0.1 nm s^{-1} for LiF (1 nm) and 0.6 nm s^{-1} for Al (100 nm). The dimensionalities of each pixel were 0.3×0.3 cm^2. After deposition, the devices were transferred to glove box and encapsulated with glass cover slips and epoxy glue. The spectra and CIE coordinates were measured using a PR655 spectra colorimeter, under ambient conditions. The current density-voltage-brightness curves were measured using a Keithley 4200 source meter and a calibrated silicon photodiode. EL transient spectra were measured with Edinburgh FLS1000 equipped with a Tektronix AFG3022G function generator. The driving voltage was 5 V. The pulse width was 20 μs.

Thermal Properties

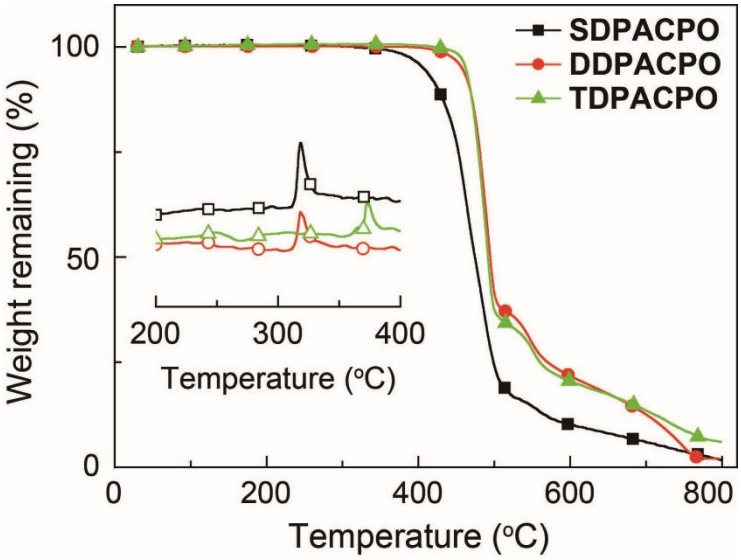

Figure S1. Thermo-Gravimetric Analysis (TGA) and Differential Scanning Calorimetry (DSC) curves of **SDPACPO**, **DDPACPO** and **TDPACPO**.

Gaussian Simulation Results

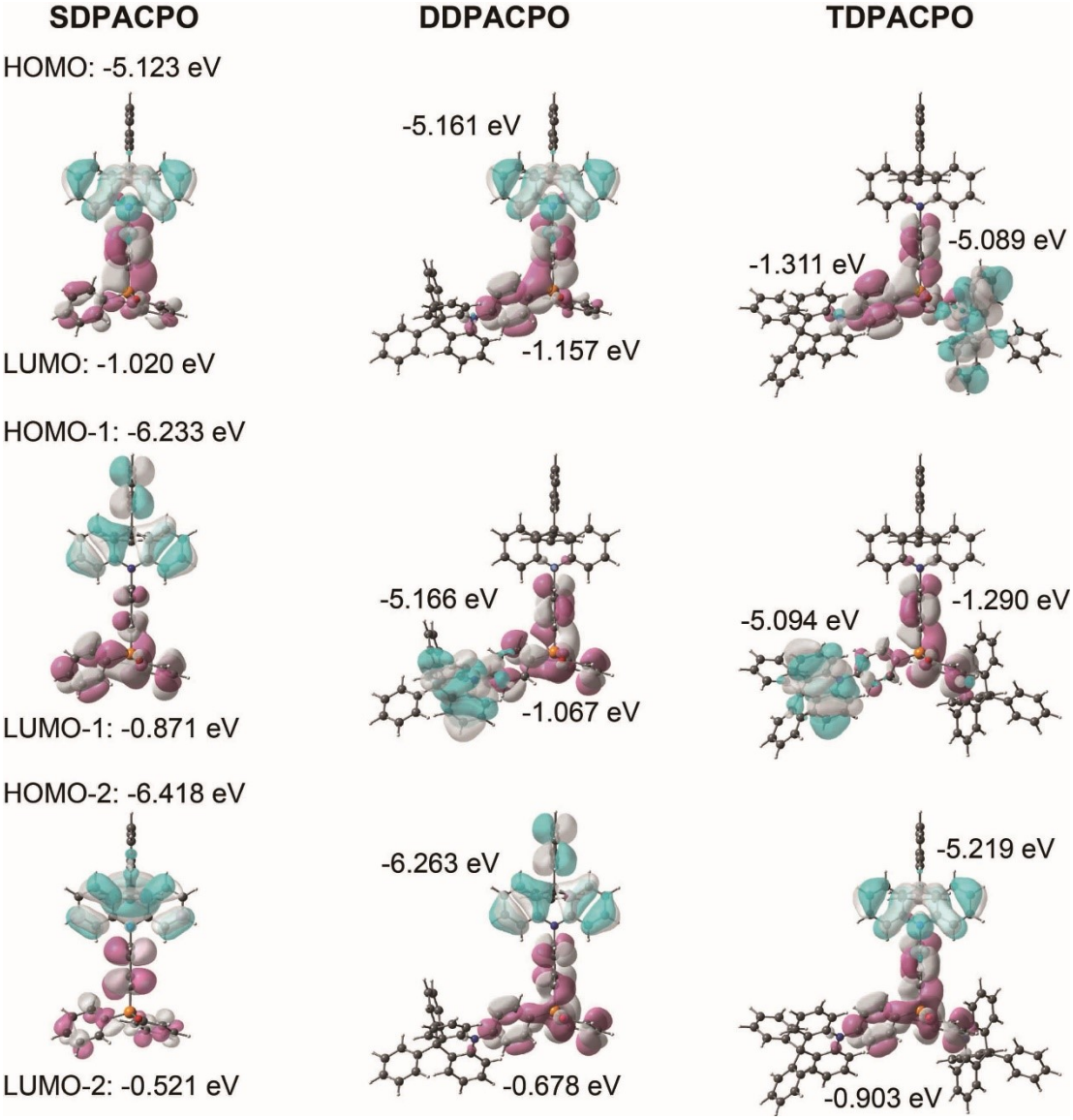

Figure S2. Contours and energy levels of occupied (cyan) and unoccupied (pink) molecular orbitals for **SDPACPO**, **DDPACPO** and **TDPACPO**.

Steady-State Photophysical Properties

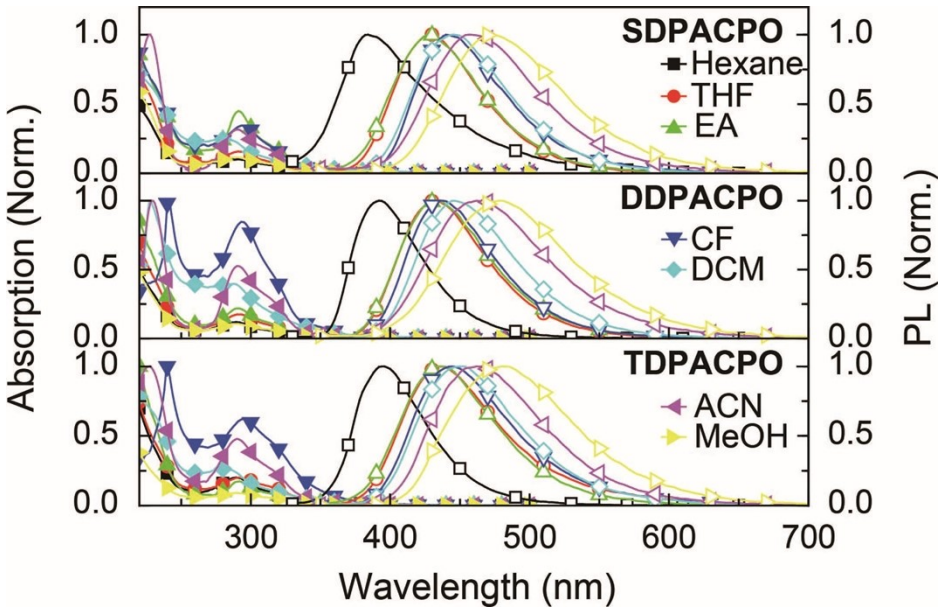

Figure S3. Electronic absorption and PL spectra of **SDPACPO**, **DDPACPO** and **TDPACPO** in solvents with different polarities (10^{-6} mol L^{-1}).

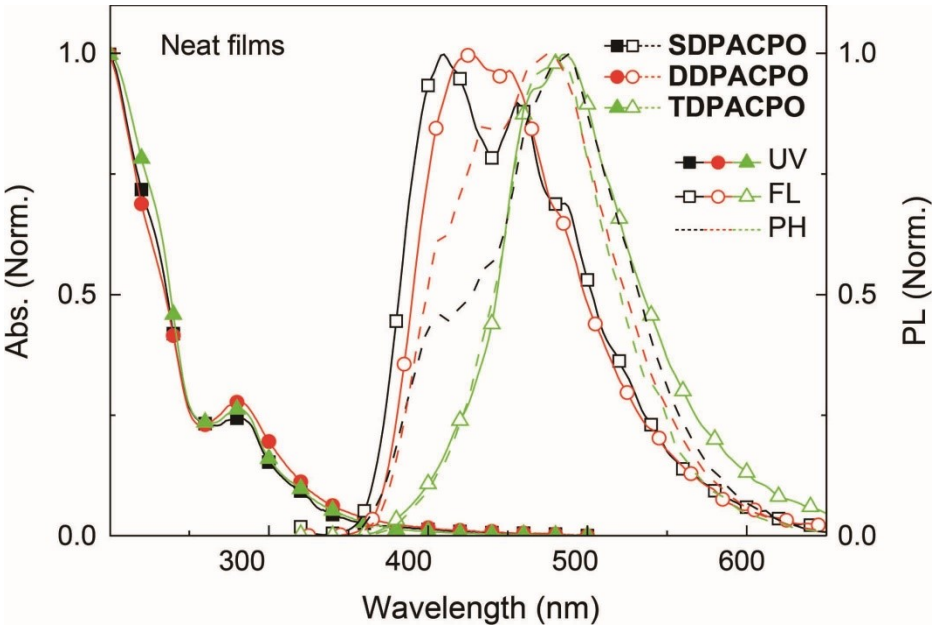

Figure S4. Electronic absorption and PL spectra of **SDPACPO**, **DDPACPO** and **TDPACPO** neat films.

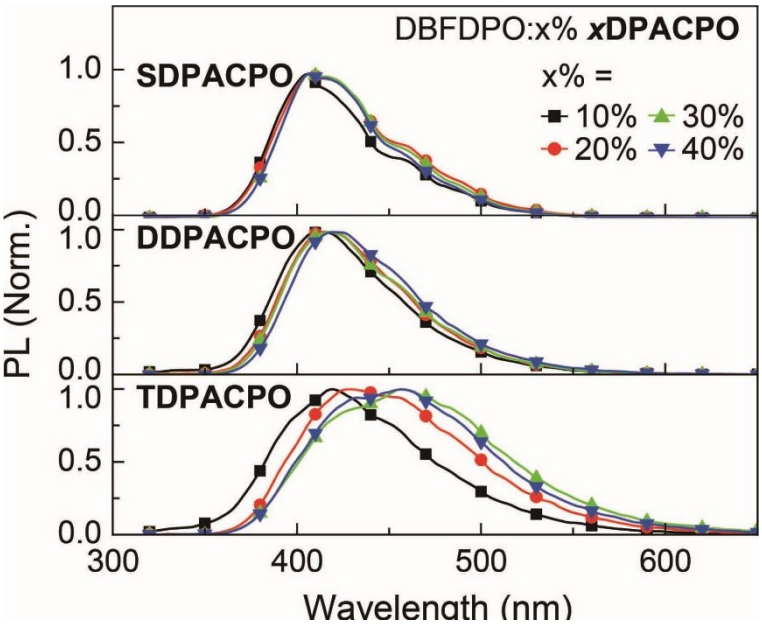

Figure S5. PL spectra of DBFDPO:x% **xDPACPO** films (x = 10, 20, 30 and 40).

Transient Emission Properties

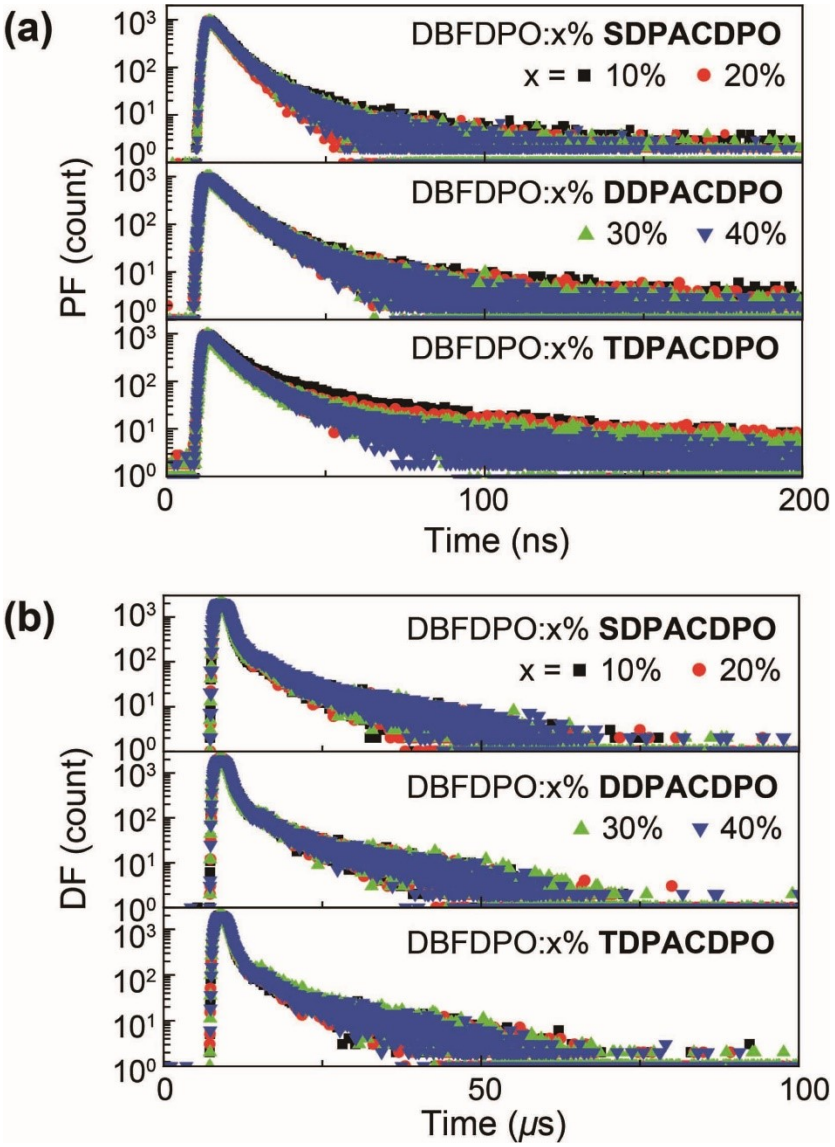

Figure S6. PF and DF time decay curves of DBFDPO:x% ***x*DPACPO** films (x = 10, 30, 30 and 40).

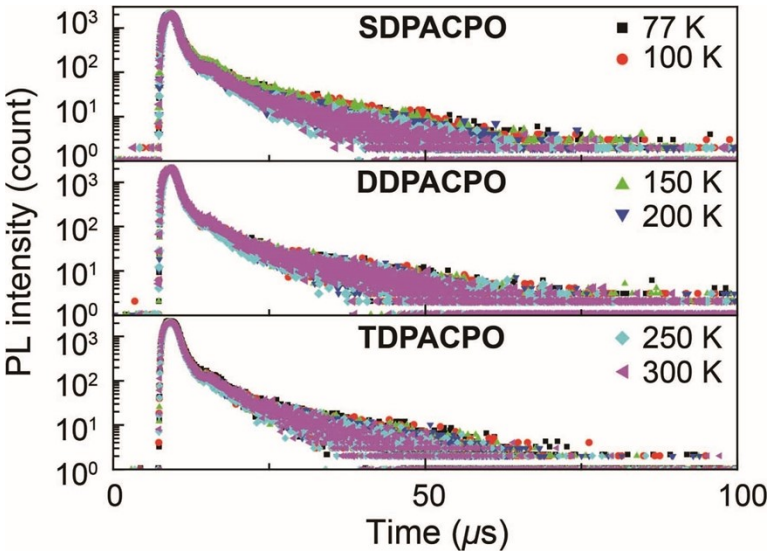

Figure S7. DF time decay curves of DBFDPO:30% ***x*DPACPO** films at range of 77-300 K.

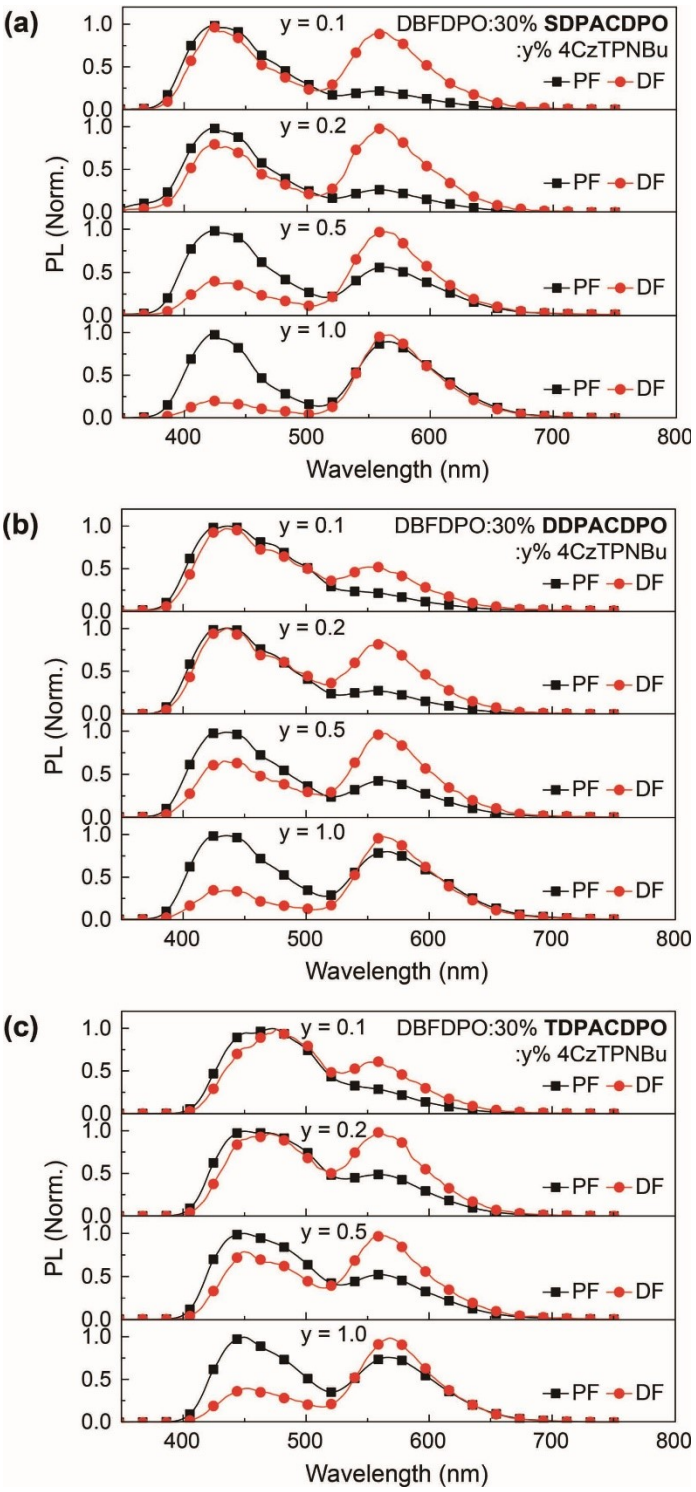

Figure S8. Prompt fluorescence (PF) and DF spectra of DBFDPO:30% **xDPACPO**:y% 4CzTPNBu films (y = 0.1, 0.2, 0.5 and 1.0). **(a)** for **SDPACPO**, **(b)** for **DDPACPO** and **(c)** for **TDPACPO**.

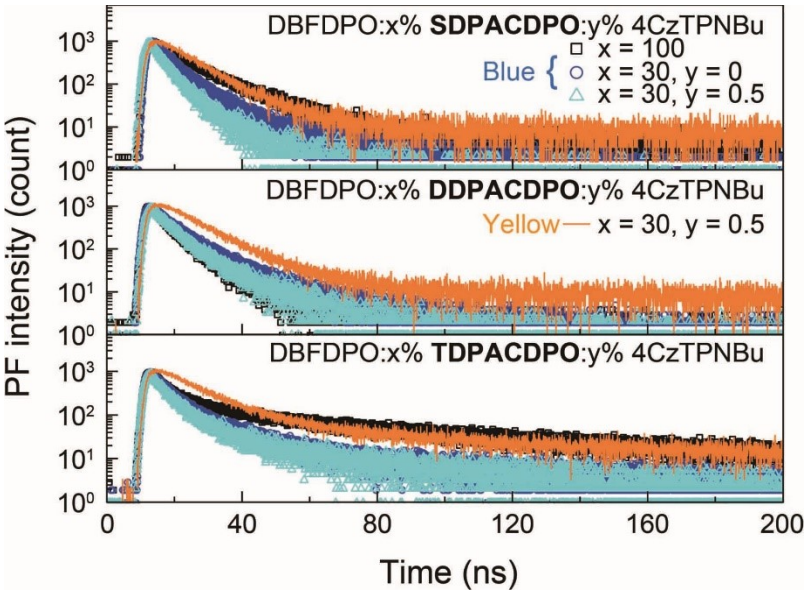

Figure S9. Comparison on PF time decay curves of DBFDPO:x% **xDPACPO**:y% 4CzTPNBu films with different x and y values.

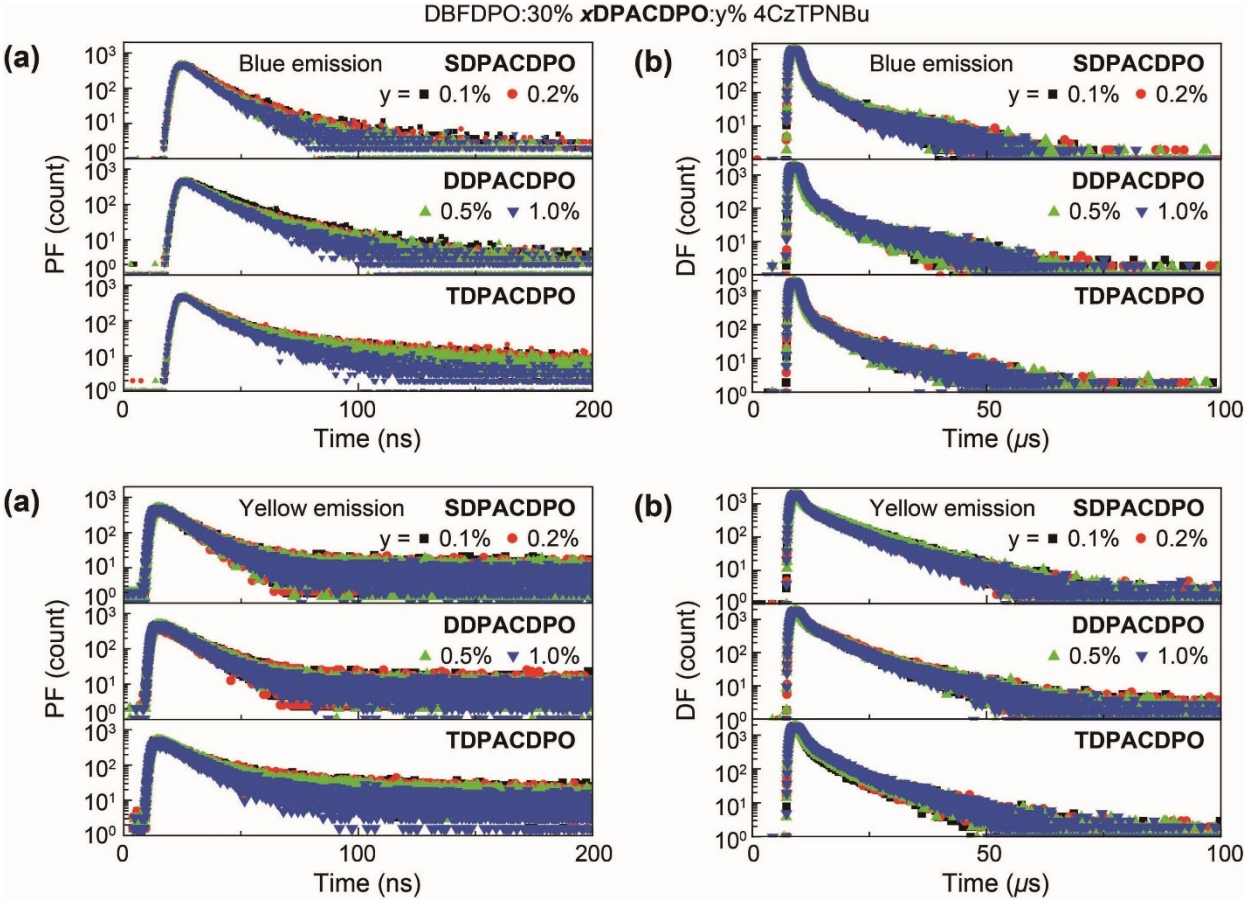

Figure S10. PF (**a** and **c**) and DF (**b** and **d**) time decay curves of blue (**a** and **b**) and yellow (**c** and **d**) emissions from DBFDPO:30% **xDPACPO**: y% 4CzTPNBu films (y = 0.1, 0.2, 0.5 and 1.0).

Electrical Properties

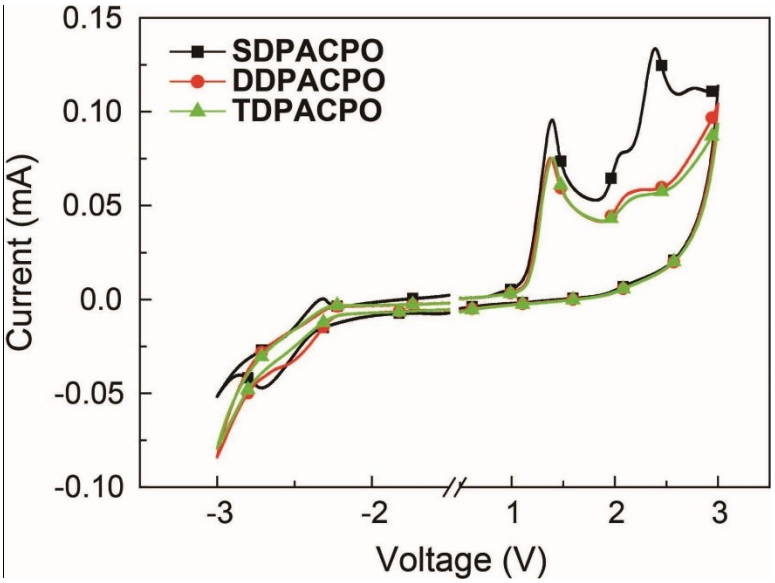

Figure S11. CV curves of **SDPACPO**, **DDPACPO** and **TDPACPO** measured at room temperature with the scanning rate of 100 mV s^{-1}.

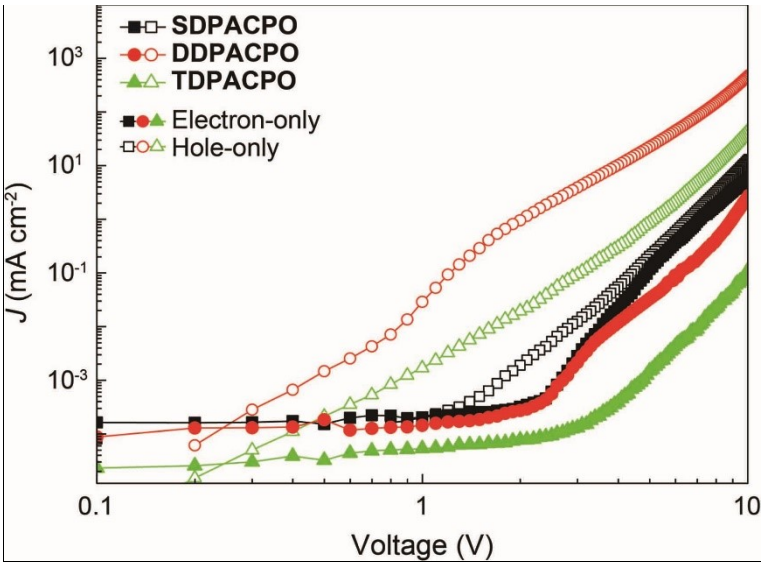

Figure S12. *I-V* characteristics of nominal single-carrier-only devices based on **SDPACPO**, **DDPACPO** and **TDPACPO** with the structures of ITO|MoO_3 (5 nm)|***x*DPACPO** (100 nm)|MoO_3 (5 nm)|Al for hole-only and ITO|LiF (1 nm)|***x*DPACPO** (100 nm)|LiF (1 nm)|Al for electron-only.

Table S1. Physical properties of ***x*DPACPO**.

TADF dye	$\lambda_{Abs.}$ (nm)	λ_{PL} (nm)	S_1 (eV)	T_1 (eV)	ΔE_{ST}[d] (eV)	T_d / T_m (°C)	HOMO (eV)	LUMO (eV)
SDPACPO	283, 228[a]	446[a]	3.18[a]	3.12[a]	0.06[a]	406/318[e]	-5.91[f]	-2.45[f]
	282, 228[b]	410, 456,	3.42[b]	3.38[b]	0.04[b]		-5.12[c]	-1.02[c]
		486[b]	3.38[c]	3.32[c]	0.06[c]			
DDPACPO	282, 228[a]	446[a]	3.14[a]	3.09[a]	0.05[a]	457/318[e]	-5.91[f]	-2.53[f]
	283, 227[b]	427, 451,	3.35[b]	3.31[b]	0.04[b]		-5.16[c]	-1.16[c]
		485[b]	3.32[c]	3.28[c]	0.04[c]			
TDPACPO	281, 228 [a]	452 [a]	3.14[a]	3.07[a]	0.07[a]	462/373[e]	-5.92[f]	-2.53[f]
	283, 228 [b]	431, 464,	3.25[b]	3.22[b]	0.03[b]		-5.09 [c]	-1.31[c]
		486 [b]	3.11[c]	3.09[c]	0.02[c]			

[a] In dichloromethane solution (10^{-6} mol L^{-1}); [b] in film; [c] Gaussian simulation results of single molecules; [d] singlet-triplet splitting; [e] temperature at weight loss of 5%; [f] calculated according to cyclic voltammetric results.

Table S2. Photophysical properties of DBFDPO:30% ***x*DPACPO** films.

Emitter	ϕ_{PL}[a] (%)	τ_{PF}[b] (ns)	τ_{DF}[c] (μs)	ϕ_{PF}[d] (%)	ϕ_{DF}[e] (%)	k_{PF}[f] (10^7 s^{-1})	k_{DF}[g] (10^3 s^{-1})	k_{ISC}[h] (10^6 s^{-1})	k_{RISC}[i] (10^3 s^{-1})	$k_{r[j]}^{S}$ (10^6 s^{-1})	ϕ_{ISC}[k] (%)	ϕ_{RISC}[l] (%)
SDPACPO	17	7.5	11.6	15	2	2.0	1.9	2.6	2.2	3.0	13	58
DDPACPO	21	9.6	11.3	18	3	1.9	2.4	2.5	2.8	3.5	13	59
TDPACPO	33	11.3	11.7	29	4	2.6	3.4	3.1	3.9	7.5	12	63

[a] PLQY measured with integrating sphere; [b] PF lifetime; [c] DF lifetime; [d] PF quantum efficiency; [e] DF quantum efficiency; Rate constants of PF[f], DF[g], intersystem crossing (ISC)[h], reverse intersystem crossing (RISC)[i] and singlet radiation[j]; [k] ISC efficiency; [l] RISC efficiency.

OLED Performance

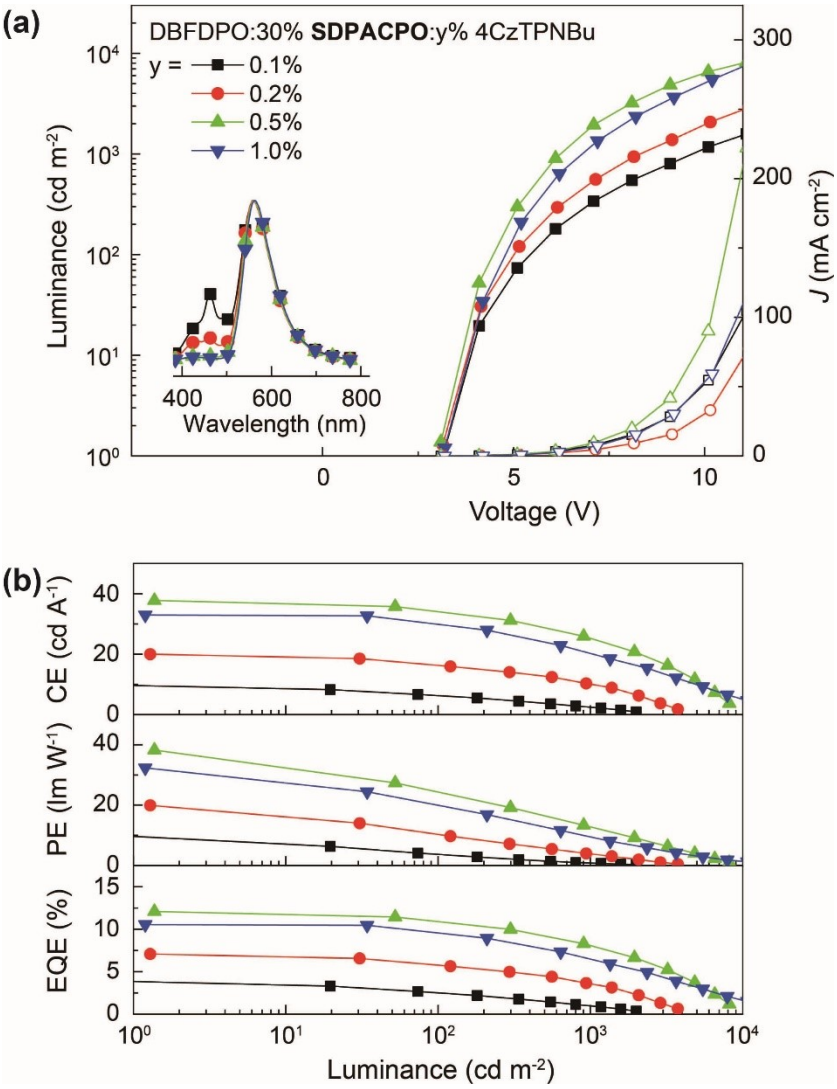

Figure S13. Device performance of white TADF diodes based on **SDPACPO** dependent on the doping concentration of 4CzTPNBu. (a) Electroluminescent spectra (insets) at 1000 nits and luminance-voltage-current density (*J*) relationships; (b) Efficiency-luminance relationships.

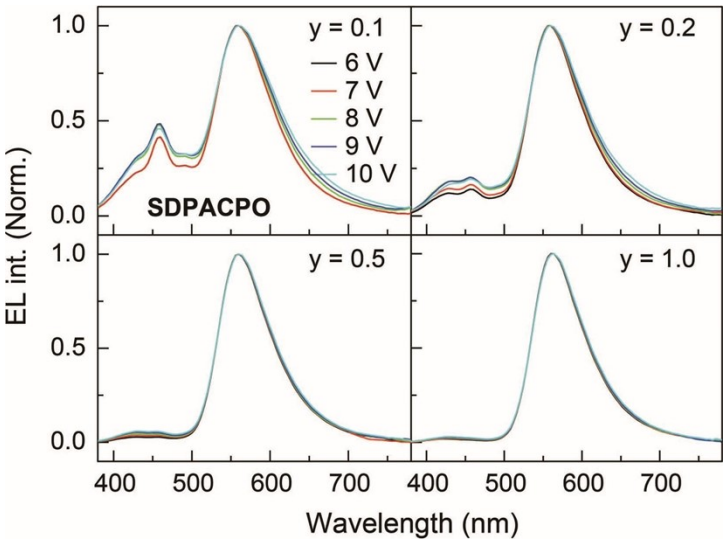

Figure S14. Electroluminescent spectral stability during voltage increasing from 6 to 10 V of **SDPACPO** based white TADF diodes.

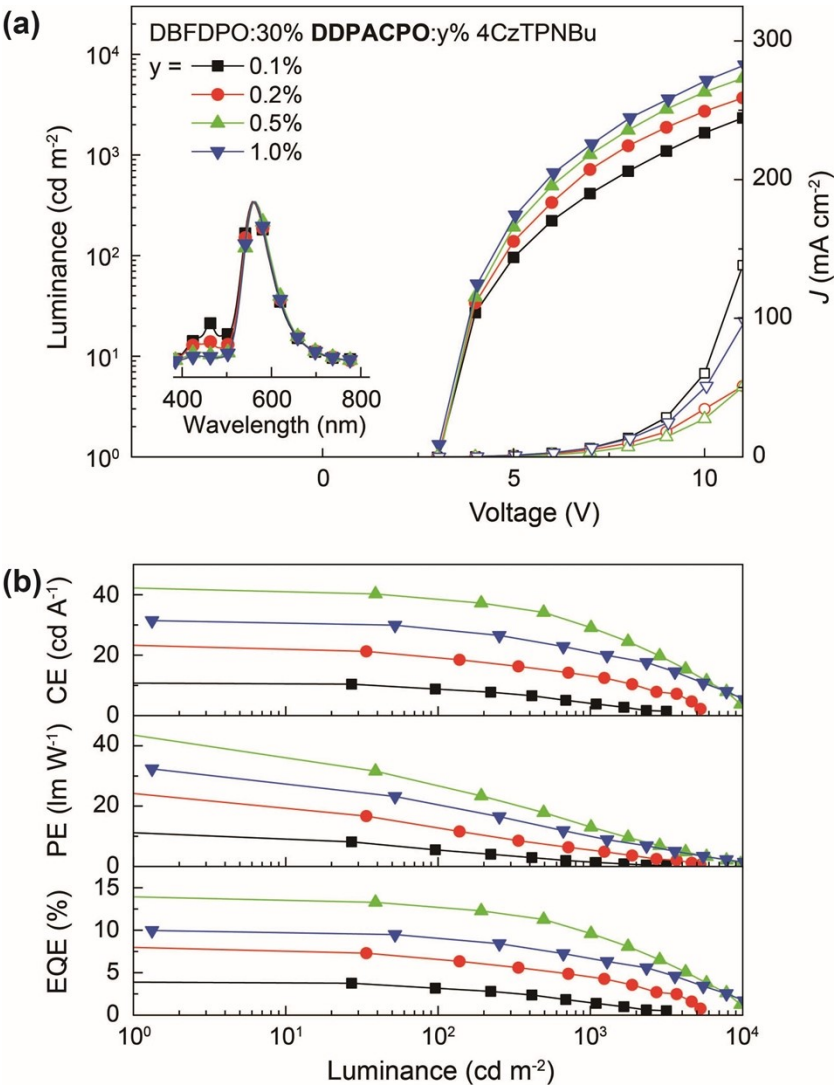

Figure S15. Device performance of white TADF diodes based on **DDPACPO** dependent on the doping concentration of 4CzTPNBu. (a) Electroluminescent spectra (insets) at 1000 nits and luminance-voltage-current density (*J*) relationships; (b) Efficiency-luminance relationships.

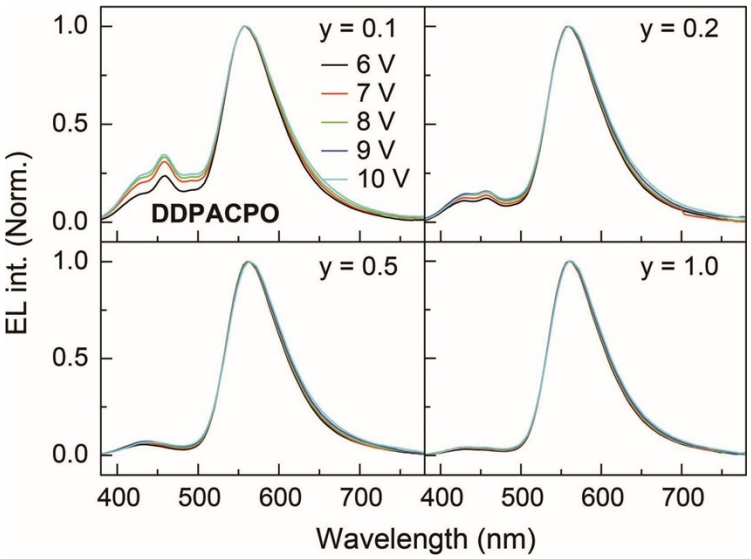

Figure S16. Electroluminescent spectral stability during voltage increasing from 6 to 10 V of **DDPACPO** based white TADF diodes.

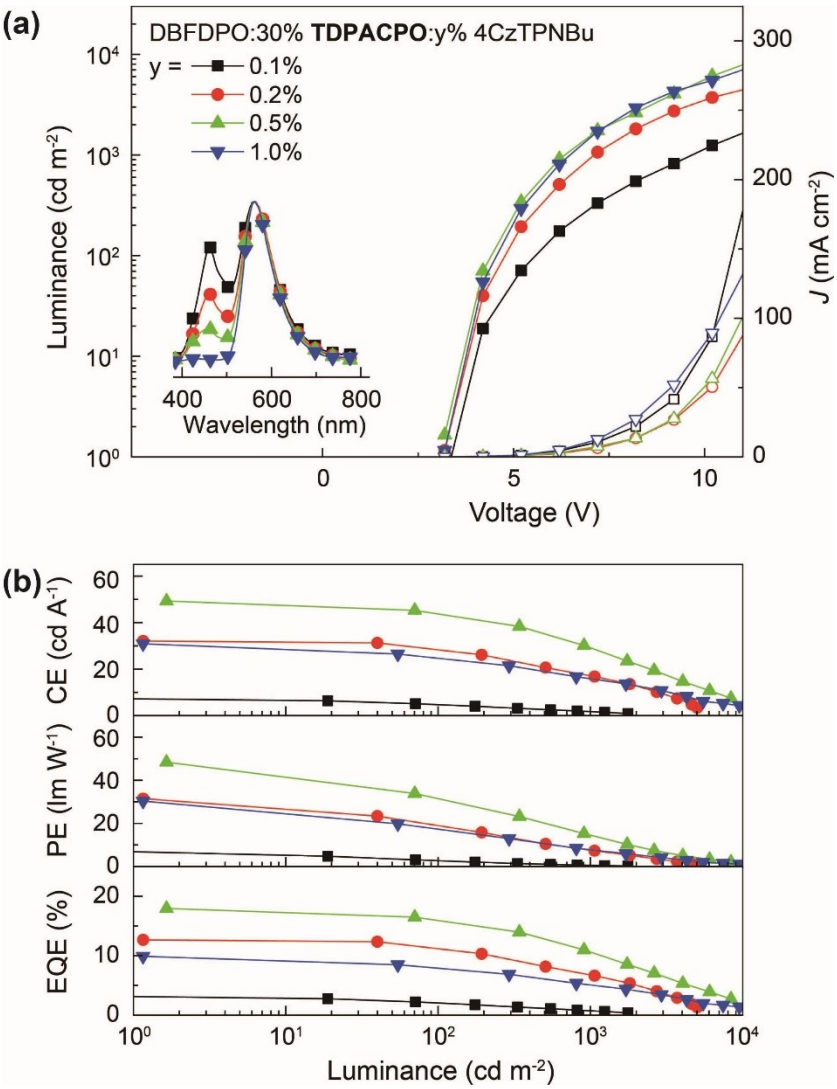

Figure S17. Device performance of white TADF diodes based on **TDPACPO** dependent on the doping concentration of 4CzTPNBu. (a) Electroluminescent spectra (insets) at 1000 nits and luminance-voltage-current density (*J*) relationships; (b) Efficiency-luminance relationships.

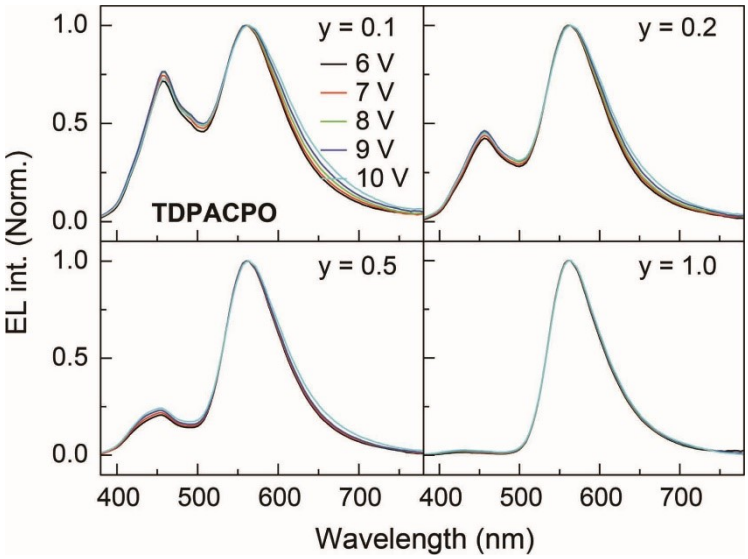

Figure S18. Electroluminescent spectral stability during voltage increasing from 6 to 10 V of **TDPACPO** based white TADF diodes.

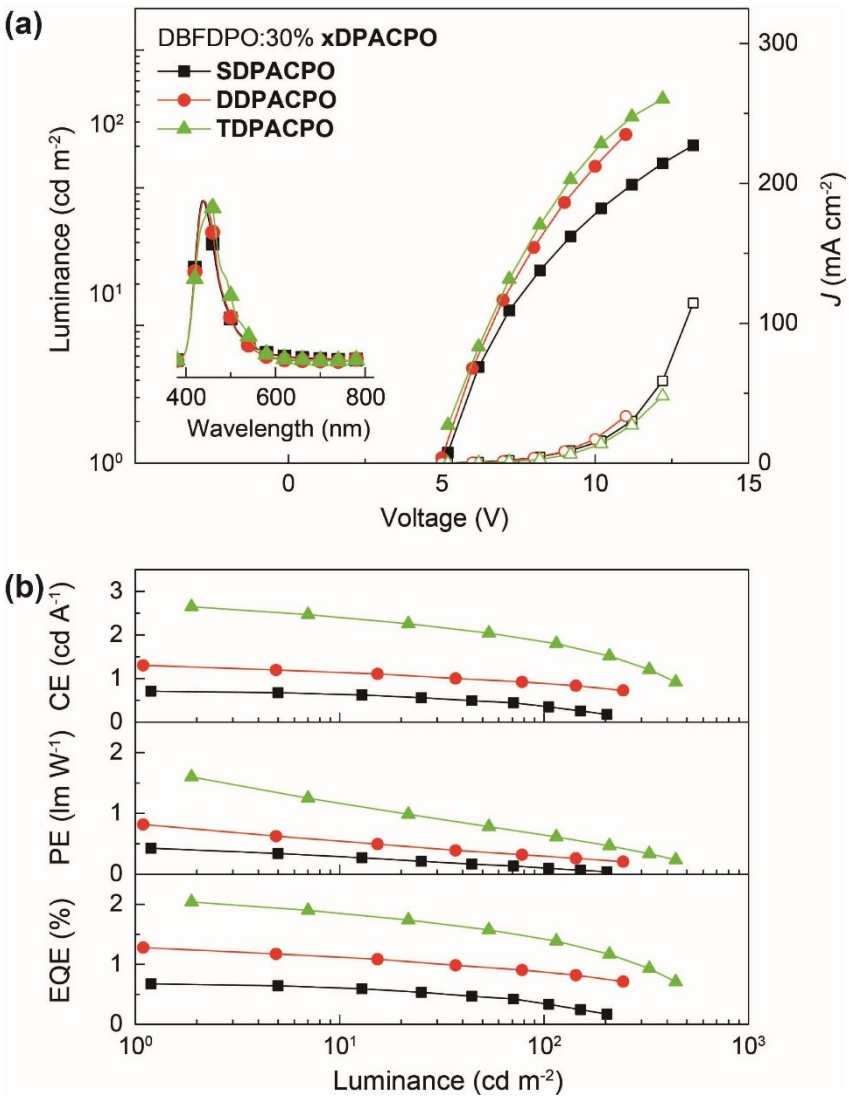

Figure S19. Device performance of blue TADF diodes based on ***x*DPACPO**. (a) Electroluminescent spectra (insets) and luminance-voltage-current density (*J*) relationships; (b) Efficiency-luminance relationships.

Table S3. EL performance of TADF WOLEDs based on ***x*DPACPO**.

Emissive layer	*y* (%)	$V^{[a]}$ (V)	$L_{max}^{[b]}$ (cd m^{-2})	$\eta^{[c]}$			CIE (x, y)[d]
				η_{CE} (cd A^{-1})	η_{PE} (lm W^{-1})	η_{EQE} (%)	
DBFDPO:30% **SDPACPO**: *y*% 4CzTPNBu	0.1	3.1, 5.2, 10.1	2000	9.7, 6.6, 2.1	9.8, 4.1, 0.7	3.9, 2.6, 0.9	(0.37, 0.43)
	0.2	3.1, 5.1, 8.1	3753	20.0, 16.0, 10.3	19.9, 9.8, 4.0	7.1, 5.7, 3.6	(0.41, 0.49)
	0.5	3.1, 4.5, 6.1	8168	37.8, 35.7, 25.9	38.3, 27.3, 13.3	12.1, 11.4, 8.2	(0.44, 0.53)
	1.0	3.2, 4.7, 6.4	13440	33.0, 32.6, 22.8	32.3, 24.4, 11.5	10.5, 10.4, 7.3	(046, 0.52)
DBFDPO:30% **DDPACPO**: *y*% 4CzTPNBu	0.1	3.1, 5.0, 8.9	3156	10.8, 8.8, 3.9	11.3, 5.5, 1.4	3.9, 3.1, 1.4	(0.39, 0.47)
	0.2	3.0, 4.9, 7.5	5285	23.3, 18.5, 12.5	24.4, 11.6, 4.9	8.0, 6.4, 4.3	(0.42, 0.49)
	0.5	3.1, 4.7, 7.0	11064	42.4, 38.2, 29.1	44.3, 27.4, 13.1	14.0, 12.7, 9.6	(0.42, 0.49)
	1.0	3.0, 4.5, 6.9	10217	31.4, 28.2, 20.0	32.3, 19.3, 8.9	10.0, 8.9, 6.5	(0.44, 0.52)
DBFDPO:30% **TDPACPO**: *y*% 4CzTPNBu	0.1	3.3, 5.5, 9.7	1764	7.4, 4.9, 1.7	7.3, 2.7, 0.6	3.2, 2.0, 0.8	(0.33, 0.38)
	0.2	3.2, 4.9, 7.2	5033	32.1, 28.6, 16.8	31.5, 19.5, 7.3	12.7, 11.3, 6.6	(0.37, 0.42)
	0.5	3.2, 4.5, 6.3	8374	49.3, 43.3, 30.1	48.4, 30.5, 15.2	17.9, 16.4, 11.0	(0.41, 0.46)
	1.0	3.2, 4.5, 6.4	9514	30.9, 24.7, 16.7	30.3, 18.9, 8.4	9.9, 8.2, 5.3	(0.46, 0.53)

[a] At 1, 100 and 1000 cd m^{-2}; [b] the maximum luminance; [c] EL efficiencies at the maximum and 100 and 1000 cd m^{-2}; [d] peak wavelengths and CIE coordinates of EL emissions at 1000 cd m^{-2}.

References

1. Becke AD. Density-functional thermochemistry. III. The role of exact exchange. *J Chem Phys* **98**, 5648-5652 (1993).

2. Lee C, Yang W, Parr RG. Development of the Colle-Salvetti correlation-energy formula into a functional of the electron density. *Phys Rev B* **37**, 785-789 (1988).

3. Frisch MJ*, et al.* Gaussian 09. (ed^(eds). D. 1 edn. Gaussian, Inc., Wallingford CT, USA (2009).